SCHOOL OF MATERIALS AND MINERAL RESOURCES ENGINEERING
UNIVERSITI SAINS MALAYSIA

DEVELOPMENT OF PROTECTIVE OXIDE SCALES ON HASTELLOY C22 FOR HIGH TEMPERATURE CORROSION IN ALKALI SALT ENVIRONMENT

By

THOR JIN ANN

Supervisor: Dr. Tuti Katrina Bt. Abdullah

Dissertation submitted in partial fulfilment
of the requirement for the degree of Bachelor of Engineering with Honours
(Materials Engineering)

Universiti Sains Malaysia

JUNE 2017

DECLARATION

I hereby declare that I have conducted, completed the research work and written the dissertation entitled "**Development of Protective Oxide Scales on Hastelloy C22 for High Temperature Corrosion in Alkali Salt Environment**". I also declare that it has not been previously submitted for the award of any degree or diploma or other similar title of this for any other examining body or university.

Name of Student : Thor Jin Ann Signature :

Date :

Witness by

Supervisor : Dr. Tuti Katrina Bt. Abdullah Signature :

Date :

ACKNOWLEDGEMENTS

First and foremost, I would like to take this opportunity to express my utmost gratitude and appreciation to my final year project supervisor, Dr. Tuti Katrina binti Abdullah for her valuable time and effort in sharing her knowledge and experience through guidance and advice. I would like to thank Miss Syamimi binti Abu Kassim, who is a research assistant, for sharing a lot of analytical skills and knowledge help to accomplish this research project.

On top of that, I would like to thank Universiti Sains Malaysia of School of Materials and Mineral Resources Engineering for providing sufficient resources, facilities and instruments. I am deeply grateful to all the technicians and academic staffs of School of Materials and Mineral Resources Engineering, Universiti Sains Malaysia for their assistance and cooperation provided in completing my final year project.

Last but not least, I would also mention the endless motivation and support from my family and friends throughout this project. Their understanding and stimulating discussions of ideas have indirectly helped enabled the completion of this project.

TABLE OF CONTENT

LIST OF TABLES

LIST OF FIGURES

LIST OF ABBREVIATIONS

AGW	Agricultural Waste
CFB	Circulating Fluidized Boiler
CFD	Computational Fluid Dynamics
DI	Deionised
EDX	Energy Dispersive X-Ray Spectroscopy
FESEM	Field Emission Scanning Electron Microscopy
HCl	Hydrochloric Acid
HVOF	High Velocity Oxygen Fuel
OM	Optical Microscope
P.O.P	Plaster of Paris
PVC	Polyvinyl Chloride
SE	Secondary Electron
XRD	X-ray Diffraction
μm	Micron meter

LIST OF SYMBOLS

%	Percentage
℃	Degree Celsius
wt%	Weight Percent
θ	Theta
λ	Wavelength

PENGHASILAN LAPISAN OKSIDA PELINDUNG ATAS HASTELLOY C22 UNTUK KAKISAN SUHU TINGGI DALAM PERSEKITARAN GARAM AKALI

ABSTRAK

Kakisan suhu tinggi yang disebabkan oleh klorin pada suhu tinggi adalah kelemahan utama pengkomersilan penjanaan kuasa melalui biojisim Untuk melindungi aloi, kelakuan pengoksidaan Hastelloy C22 telah dikaji dengan menghasilkan lapisan oksida pelindung di atas permukaan Hastelloy C22 pada suhu yang berbeza (800, 900, 1000 dan 1100 ℃). Produk pengoksidaan telah dikaji secara terperinci melalui Mikroskop Elektron Pengimbas dilengkapi dengan Serakan Tenaga X-ray Spektroskopi (FESEM-EDX), X-ray Pembelauan (XRD) dan ukuran peningkatan jisim. Hasilan lapisan oksida pelindung telah berjaya terbentuk di atas Hastelloy C22 yang dipra-oksidakan pada 1000 ℃. Kemudian, kelakuan kakisan Hastelloy C22 dengan lapisan oksida pelindung dan tanpa lapisan oksida pelindung dalam persekitaran garam alkali yang mengandungi 95.5 wt% KCl + 4.5 wt% NaCl telah dibandingkan dan dikaji. Ujian kakisan telah dijalankan pada suhu 700 ℃ selama 100 jam. Produk kakisan telah diperiksa melalui pencirian yang sama seperti produk pengoksidaan, kecuali ukuran peningkatan jisim yang telah digantikan dengan ukuran kehilangan jisim. Hal ini disebabkan oleh perkecaian lapisan oksida di atas Hastelloy C22. Hastelloy C22 yang dipra-oksidakan mempunyai rintangan kakisan yang lebih baik berbanding dengan Hastelloy C22 yang mentah kerana lapisan oksida tersebut mempunyai keupayaan untuk menghalang penembusan bahan kakisan ke dalam substrat.

DEVELOPMENT OF PROTECTIVE OXIDE SCALES ON HASTELLOY C22 FOR HIGH TEMPERATURE CORROSION IN ALKALI SALT ENVIRONMENT

ABSTRACT

High temperature corrosion is the major drawback of commercialization of biomass fired power generation due to the chlorine-induced corrosion at high temperature. In order to protect the underneath alloy, the oxidation behavior of Hastelloy C22 at different temperatures (800, 900, 1000 and 1100 ℃) was studied in order to develop a protective oxide scale. The oxidation products were investigated in detail via Field Emission Secondary Electron Microscope equipped with Energy Dispersive X-ray Spectroscopy (FESEM-EDX), X-ray Diffraction (XRD) and mass gain measurement. From the results, the protective oxide scale was successfully developed on Hastelloy C22 that was pre-oxidised at 1000 ℃. Then, the corrosion behavior of Hastelloy C22 with protective oxide scale and without protective oxide scale in alkali salt environment consisting of 95.5 wt% KCl + 4.5 wt% NaCl were compared and studied. The corrosion test was conducted at 700 ℃ for 100 hours. The corrosion products were examined via the same characterization as oxidation products, except for the mass gain measurement which was replaced by mass loss measurement due to the spallation of oxide scale. The pre-oxidised Hastelloy C22 exhibits better corrosion resistance than the raw Hastelloy C22 as the oxide scale formed has the ability to prevent the penetration of corrosion reagent into the substrate.

CHAPTER 1

INTRODUCTION

1.1 Background

The world concerns about the environmental issues especially related to the use of fossil fuels. Thus, people are continuously searching for alternatives to reduce the greenhouse gas effect (Khan et al., 2009). Biomass power generation is believed to be an attractive alternative to fossil fuels because combustion of biomass produces no net contribution of CO_2 to the atmosphere. However, corrosion of the construction materials of biomass boilers and superheaters is the major drawback when generating electricity from biomass combustion. Hence, the biomass-fired energy plants normally operated at a considerably lower temperature between 450 ℃ and 650 ℃ in order to limit the degradation of the superheater (Viklund et al., 2013, Luo et al., 2012). As a consequence, the efficiency of the power generation is greatly diminished.

Recently, the biomass power generation industry has been progressively shifting towards higher operating steam temperatures and pressures due to the desire of increasing the electricity generation efficiency of the biomass fired plants. However, higher operating temperature introduces potential high temperature corrosion problems and leads to more aggressive corrosion of the boiler components, for example, active oxidation induced by chlorine, sulfidation, and molten salt attack (Otsuka, 2011). Corrosion problems may result in superheater tube leakage, undesired boiler shutdowns, and shortened service life of the boiler tubing. These are very severe consequences of corrosion and may cause high maintenance cost (Oksa et al., 2013).

Chlorine induced corrosion is considered the major cause for rapid corrosion attack. The corrosion mechanisms are usually related to chlorine-rich deposits. Chlorine in the deposits is combined with alkali metals to form chlorides. It has been observed that chlorine deposits are highly corrosive when temperatures of metal exceeded 450 ℃. Therefore, high contents of alkali metals and chlorine in biomass fuels may have negative effect on the performance of the plant (Capablo, 2016). The rapid corrosion attack can be explained by a so-called active oxidation mechanism whereby gaseous chlorine (Cl_2) is formed from deposit and flue gas. The chlorine gas may continuously react with metal alloy and being released into the environment. This chlorine cycle is repeated and hence the oxidation of the metal alloy cannot be prevented. Besides, molten salts, such as chloride and sulphate salt, are also one of the major causes for rapid corrosion as they can dissolve the oxide scales and accelerate the corrosion rate (Viklund et al., 2013).

As a result, it is necessary to improve the corrosion resistance of the alloys in order to increase the operating steam temperature in biomass-fired plants (Pettersson et al., 2011). This can be achieved through alloy modification. Rapid corrosion is commonly observed in iron-based or superheater alloys with 1 – 2 % chromium (Cr), while higher alloyed steels such as austenitic stainless steels or nickel based alloys showed higher corrosion resistance (Viklund et al., 2013).

Hastelloy C22 is a candidate material for biomass boilers. It is a nickel based alloy and typically consists of 22 % chromium, 14 % molybdenum, and 3 % tungsten. Its iron content is normally limited to be lower than 3 %. Hence, Hastelloy C22 exhibits excellent resistance to corrosive attack by seawater under stagnant and flowing conditions. At elevated temperatures, the high chromium content of Hastelloy C22 helps

it to resist oxidation, carburization, and sulfidation. Since it is nickel based, it resists high temperature attack by halides (e.g. chlorides and fluorides). Furthermore, chromia layer can act as protective oxide scales to the underneath metal. Some studies also stated that the metal alloy must consists of a minimum 10 – 20 % chromium in order to ensure the chromia formation (Kofstad, 1988, Croll & Wallwork, 1969). Thus, the protective chromia layer is believed to be produced on the surface of Hastelloy C22.

The problem of high temperature corrosion has to be resolved so that to ease the commercialization of biomass fired power generation. Therefore, the optimum temperature of the pre-oxidation has to be identified in order to develop protective oxide scales on Hastelloy C22.

1.2 Problem Statement

According to the work from Luo et al. (2012), the corrosion behaviors of three different materials, which are 20#steel, TP347H and superalloy C22, have been investigated. The three different materials are having different Ni-Cr content from low to high. In the study, the materials were tested with alkali salt environment under normal oxidising environment at temperature of 650 ℃ for 218 hours. Through performing test on the mass loss measurement and Scanning Electron Microscopy (SEM) on the corrosion products, it has been concluded that superalloy C22 is the most corrosion resistant among three materials due to its highest Ni-Cr content. The oxide scale formed on the superalloy C22 is fine and light which is believed to have the ability to prevent the penetration of chlorine into the alloy surface.

In the previous works, information regarding the corrosion behavior of superalloy C22 under normal oxidising atmosphere can be obtained (Liu et al., 2014,

Luo et al., 2012). The corrosion behavior of pre-oxidised superalloy C22 is of the great interest now because the nature of the surface layers produced on the metal will play a major role in the behavior of the material in corrosive environment. The selective oxidation of elements that form a slowly growing and protective scale is the basis for the oxidation protection of all alloys used at high temperature. Cr is one of the elements that consistently result in protective scales, which is chromia scale (Birks et al., 2006). Therefore, in this work, a layer of protective oxide scale is first developed prior to the expose of superalloy C22 to the alkali salt environment instead of directly expose the alloy to the alkali salt environment. Thus, the comparison between corrosion behaviour of raw superalloy C22 and pre-oxidised superalloy C22 can be studied.

1.3 Research Objectives

Objectives of this research are as follows:

i. To study the oxidation behaviour of Hastelloy C22 after the pre-oxidation treatment.
ii. To determine the optimum temperature for the development of protective oxide scale on Hastelloy C22.
iii. To compare the corrosion behavior of raw and pre-oxidised Hastelloy C22 under the same corrosion conditions.

1.4 Research Scope

This research covered the study on protective oxide scales development and the corrosion behaviour of raw and pre-oxidised sample in the same alkali salt environment and same temperature. To develop protective oxide scales, the samples underwent isothermal corrosion at four different temperatures (i.e. 800, 900, 1000 and 1100 ℃) for 4 hours. An optimum temperature was chosen to develop the oxide scales based on the surface morphology, thickness of oxide layer and phase present in the oxide layer. Then, the raw and the pre-oxidised samples were completely immersed in the salt containing 95.5 wt% KCl and 4.5 wt% NaCl at 700 ℃ for 100 hours. Optical Microscope (OM) and X-ray Fluorescence (XRF) were used to characterize the micrograph and elemental composition of raw sample. The surface morphology, elemental distributions of corrosion products were examined using a Field Emission Scanning Electron Microscope equipped with Energy Dispersive X-ray (FESEM-EDX). X-ray Diffraction (XRD) was utilized in phase identification of corrosion layers. Furthermore, mass gain and mass loss were measured to determine the corrosion resistance of samples.

1.5 Thesis Outline

This report consists of five chapters. Chapter 1 describes a brief introduction, objectives and research scope of present work. Chapter 2 provides better understanding of background literature review relevant to present work, including the review of high temperature corrosion, the mechanism of chlorine-induced corrosion, the corrosion behaviours of several materials under the attack of different corrosive species such as alkali chlorides, and the mitigation strategies. Chapter 3 details the sample preparation procedures, overall experimental procedures and characterization techniques used in this

research study. Chapter 4 presents the experimental results and comprehensive discussions on the protective oxide scales developed and the corrosion behavior of raw hastelloy C22 and pre-oxidised hastelloy C22 under the same salt concentration and temperature. Lastly, in Chapter 5, conclusion and recommendations are presented for future studies.

CHAPTER 2

LITERATURE REVIEW

2.1 Introduction

Fossil fuels are commonly used to generate energy worldwide (Antunes & de Oliveira, 2013). Through burning fossil fuels, such as coal, natural gas and oil, greenhouse gases which are not desirable are emitted, for example, carbon dioxide (CO_2) and nitrogen oxides. These greenhouse gases contribute to climate change through global warming effect. Global warming is one of the major concerns around the world and has fostered interest in CO_2-neutral energy sources for power production recently (Chiari & Zecca, 2011). Therefore, the use of biomass for electricity generation becomes a growing interest as biomass provides energy using renewable resources, reduces the dependence on imported fossil fuels and considerably reduce the environmental impact (Nunes et al., 2016).

Furthermore, biomass energy is also an attractive solution for both energy production and conservation of land, otherwise wasted in landfills (Rajor, 2011). Landfill disposal of waste may cause ground water pollution especially when the landfill site is inadequately designed or operated. In locations where population densities are high, the use of landfills for waste disposal has become less feasible and waste incineration becomes a more attractive option (Mudgal et al., 2014).

Biomass energy is an energy that is derived from living matter such as field's crops and trees. Agricultural and forestry wastes and municipal solid wastes are also considered in the biomass category. Malaysia is endowed with abundant supplies of

biomass resources. However, the main sources of biomass in Malaysia are come from plantation residue and agricultural residue. Thus, Malaysia is considered as one of the potential countries in this field (Shafie et al., 2012).

The technologies available for power generation from biomass are direct combustion, gasification and pyrolysis. The most widely used and established application is direct combustion of solid biomass. Combustion converts biomass energy into heat then electricity energy base on thermo-chemical process with output production of hot gases at temperature around 800 – 1000 ℃ (Shafie et al., 2012). However, high temperature corrosion induced by chlorine and alkali metal is a major drawback to the consolidation of this technology (Antunes & de Oliveira, 2013, Waldmann et al., 2008). This limits the temperature of the vapour and hence the effectiveness of biomass plant (Ruiz & Berlanga, 2013). Figure 2.1 shows the formation of corrosive elements during biomass combustion.

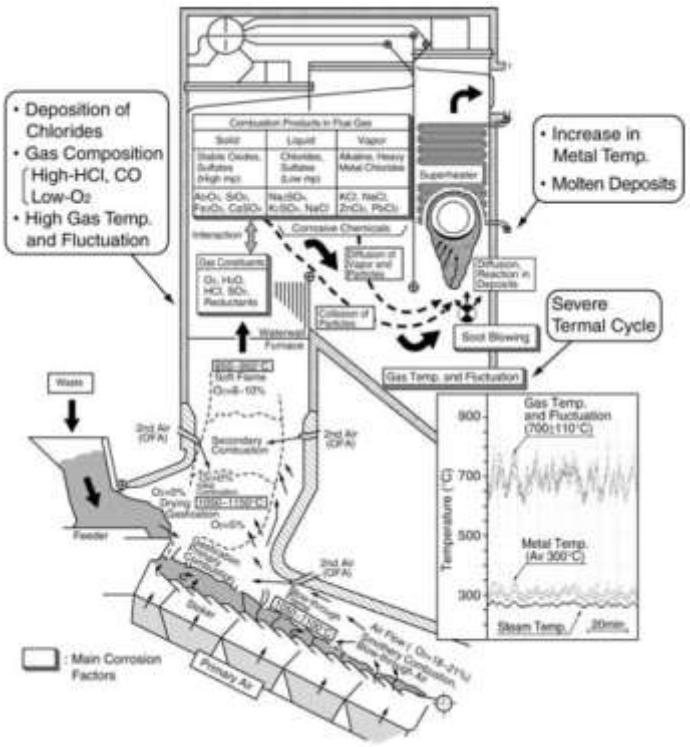

Figure 2.1: Formation of corrosion environment in boilers (Kawahara, 2007)

During the combustion of waste, the construction materials may be damaged by corrosion. High temperature corrosion that occurs during waste combustion in a boiler includes rapid scaling by sulphides, scale delamination, oxide scale fluxing due to the presence of molten salt species, internal oxidation because of the penetration of sulphur species along the grain boundaries, fouling due to heavy deposits that influence heat and mass transfer, erosion or impaction effects (Antunes & de Oliveira, 2013).

Typically, superheater tube temperature is 400 – 650 ℃. Due to localised overheating, the tube heat exchange surface temperature may be above 700 ℃. However, in order to improve electrical efficiency of biomass combustion plants, superheated steam temperature has to be increased. But, higher temperature contributes to higher amount of molten phases in deposits and vapour phases in the flue gas (Liu et al., 2014). As a result, the corrosion of superheater tubes is aggravated. It is common for biomass boilers to have a high corrosion rate when metal temperatures exceed 500 ℃ (Chen et al., 2012). This attributes to a number of corrosion mechanisms coexist and may occur simultaneously. Skrifvars et al. (2008) also stated that a steam temperature above 500 ℃ may result severe corrosion in short time span.

Johansson et al. (2007) highlighted that superheaters corrosion is an important obstacle to the development of biomass as a competitive alternative source for "green energy". The corrosion of superheater tubes can be related to the material as well as the chemical composition of deposits formed on the tubes (Nielsen et al., 2000). Hence, in order to protect the construction materials from the high temperature corrosion, the mechanism of the corrosion needs to be studied and the corrosion resistance of different material has to be investigated.

2.2 Corrosion Mechanism

Biomass composition plays a pivotal role in the combustion process. Inorganic elements such as chlorine, sodium, potassium, sulfur, nitrogen, phosphorus, calcium, magnesium and silicon always present in the biomass boiler. Biomass fuels are also rich in alkali metals (K and Na). They usually appear in the form of simple salts, organic compounds or chlorine (Nielsen et al., 2000). These species are promptly released to the gas phase during combustion and formed hydrochloric acid (HCl) and potassium chloride (KCl). Mudgal et al. (2014) also stated that waste combustion can result in generation of chlorides of sodium and potassium that may attack the metallic part in boilers.

Ash is formed during combustion from inorganic, ash-forming components. There are two types of ash, which are bottom ash and fly ash. Fly ash particles, that are formed form gas phase ash-forming compounds, typically are mainly alkali metal chlorides and sulfates. These particles influences heat transfer in furnace and initiates deposit formation that causes corrosion on superheater tubes (Lind et al., 2006).

2.2.1 Role of Alkali Chlorides

Alkali chlorides are formed when alkali metal oxides react with HCl. They can condensate and form deposits on metal surface which leads to the corrosion of the metal. Potassium chloride (KCl) and sodium chloride (NaCl) are examples of alkali chlorides. In the research work of Enestam et al. (2013), high chromium stainless steel Sanicro 28 was exposed to both of the chlorides. When exposed to NaCl, the degraded part of Sanicro 28 was as thick as the corrosion product. The sample was affected by selective corrosion at which the steel surface contained almost solely of nickel (Ni) and

completely depleted from iron (Fe) and chromium (Cr) when exposed to NaCl at 600 ℃. While for the exposure to KCl, only minor internal degradation was observed. Although Sanicro 28 experienced higher degree of internal degradation when exposed to NaCl than to KCl, the two chlorides are equally corrosive to superheater steels when considered practical applications.

Furthermore, Luo et al. (2012) reported that high content of potassium (K) and chlorine (Cl) in deposits are potentially harmful elements with regard to the corrosion of superheater tube surfaces. Initially, chlorine and alkali metal combine into corrosive compositions in the flue gas and deposit on heat transfer surfaces through condensation of vapours, sticking to particles and chemical reactions like sintering and slagging occurred. These result in the damage of the construction materials. They also stated that the chlorine-containing ash deposits increases the corrosion rate by several mechanisms. Chlorine in the form of alkali chloride deposited on a steel surface at temperatures higher than 450 ℃ accelerates the corrosion of the steel surface (Vaughan, 1978, Grabke, 1991, Salmenoja et al., 1996). The process is called "active oxidation" whereby a "chlorine cycle" may be involved in the reaction. The main reactions involved in the active oxidation mechanism are summarized by Grabke et al. (1995) as shown in Equation (2.1) to (2.7).

$$2HCl + \frac{1}{2}O_2 \leftrightarrow Cl_2 + H_2O \quad (2.1)$$

$$2NaCl + Fe_2O_3 + \frac{1}{2}O_2 \leftrightarrow Na_2Fe_2O_4 + Cl_2 \quad (2.2)$$

$$4NaCl + Cr_2O_3 + \frac{5}{2}O_2 \leftrightarrow 2NaCrO_4 + 2Cl_2 \quad (2.3)$$

$$Fe + Cl_2 \leftrightarrow FeCl_2(s) \quad (2.4)$$

$$FeCl_2(s) \leftrightarrow FeCl_2(g) \quad (2.5)$$

$$3FeCl_2 + 2O_2 \leftrightarrow Fe_3O_4 + 3Cl_2 \quad (2.6)$$

$$2FeCl_2 + \frac{3}{2}O_2 \leftrightarrow Fe_2O_3 + 2Cl_2 \quad (2.7)$$

Reaction between condensed chloride and the oxide scales may result in the formation of chlorine through reactions (2.1), (2.2) and (2.3). As chlorine has the ability to penetrate the oxide scale through pores or cracks and react with the metal alloy, metal chlorides are then formed at the interface of metal and scale as shown in reaction (2.4). $FeCl_2$ has high vapour pressure at 500 ℃, which is the typical temperature for biomass combustion, it volatilizes according to reaction (2.5). When it diffuses through the oxide scale, oxidation occurs to produce Fe_3O_4 and Fe_2O_3, and chlorine is again released into the environment according to reactions (2.6) and (2.7). This chlorine cycle will be repeated, hence the oxidation of the metallic surface beneath the non-protective oxide scale is sustained. This active oxidation induced by chlorine can be presented in reaction circuit shown in Figure 2.2.

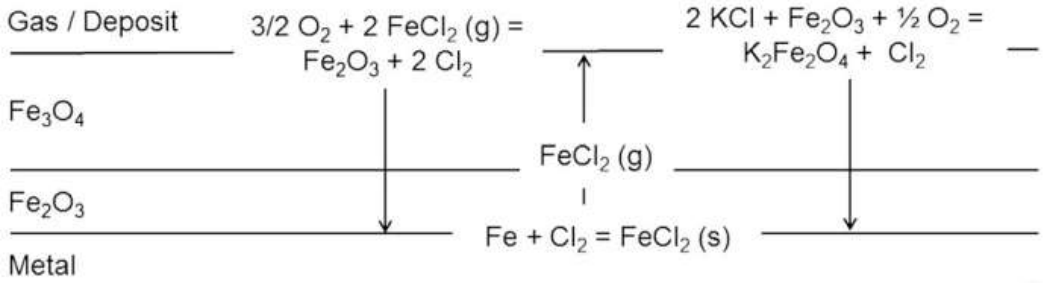

Figure 2.2: Schematic illustration of active oxidation reaction circuit. The reactions are similar to NaCl (Grabke et al., 1995)

Nielsen et al. (2000) also reported that the presence of alkali chloride in deposits may increase the oxidation well below the melting temperature of the salt. Moreover, from the work of Skrifvars et al. (2008), a very low amount of chlorine, which is 0.3 wt% in the salt, triggers the "active oxidation" corrosion mechanism especially when

potassium is present in the salt. A possible explanation to this oxidation is that potassium enhances the break-up of the protecting oxide layer on the steel surface according to Equation (2.8) and (2.9), forming some potassium–chromium compound, and leaving an easy accessible pathway for chlorine to react with the unprotected steel. This also has been investigated by Karlsson et al. (2011). Samples that were coated with KCl showed dramatic chromia (Cr_2O_3) depletion of the protective oxide due to formation of K_2CrO_4.

$$2KCl + \frac{1}{2}Cr_2O_3 + \frac{5}{4}O_2 \rightarrow K_2CrO_4 + Cl_2 \quad (2.8)$$

$$2KCl + Fe_2O_3 + \frac{1}{2}O_2 \rightarrow K_2Fe_2O_4 + Cl_2 \quad (2.9)$$

In addition, Antunes and de Oliveira (2013) also stated that high amounts of KCl in the combustion gases are frequently associated with enhanced deposit formation. This, in turn, will lead to corrosion of superheater tubes in biomass-fired boilers.

2.2.2 Role of Sulfur

Sulfur is also involved in the corrosion-related phenomena. It is readily released during the combustion. Typically, alkali metal sulfates and calcium sulfates are found in the condensed phase while sulphur dioxide (SO_2) is the main sulfur compound in the gas phase. Although the sulfation reaction in the condensed phase is slower, it is still significant in deposits (Lind et al., 2006). This reaction is likely to accelerate the corrosion processes in biomass boilers when contact with SO_2 in the gases. SO_2 reacts with alkali chlorides and HCl or Cl_2 is generated close to the metal surface through reaction (2.10) and (2.11), where M is K or Na. If the temperature of the metal surface

is high enough for molten phases to form in the deposit, the corrosion of the metal may be further enhanced (Nielsen et al., 2000).

$$2MCl + SO_2 + \frac{1}{2}O_2 + H_2O \rightarrow M_2SO_4 + 2HCl \quad (2.10)$$

$$2MCl + SO_2 + O_2 \rightarrow M_2SO_4 + Cl_2 \quad (2.11)$$

However, the thin and dense K_2SO_4 layer that formed from the sulfation reaction can act as an effective barrier to progressive corrosion in superheater tube. This layer of K_2SO_4 would prevent the gaseous chlorine species from diffusing to the metal surface. This reaction is favoured at high steam temperature of 520 ℃ (Antunes & de Oliveira, 2013).

Jiamin and Zhansong (2009) found that SO_2 had a positive effect on the corrosion behavior of a 316L stainless superheater tube in a biomass boiler operating at 500 ℃. This result was explained by the formation of the less aggressive K_2SO_4, according to the same route shown in Equation (2.10) and (2.11). This reaction yields the formation of a compact $FeSO_4$ layer that reduces the mass gain at high temperatures. Davidsson et al. (2007) confirmed the validity of this mechanism in a commercial scale boiler. The addition of SO_2 to the burning atmosphere resulted in the K_2SO_4 formation according to Equation (2.10) and (2.11) whereas the addition of HCl shifted this accelerated corrosion of the superheater tubes by the reaction shown in Equation (2.12).

Furthermore, Karlsson et al. (2011) investigated the effect of SO_2 on the oxidation of alloy 404L in O_2+H_2O and O_2+H_2O+KCl environment. Upon the addition of SO_2, both cases showed drastic reduction of corrosion rate. In the O_2+H_2O environment, the reduction of oxidation rate is attributed to the sulphate film formation on the oxide surface which prevents chromium volatilization. While in O_2+H_2O+KCl environment, the corrosion mitigating effect is mainly due to the rapid conversion of

KCl to K_2SO_4 that does not deplete the protective chromium oxide by forming K_2CrO_4 as compared to KCl.

2.2.3 Role of Potassium Carbonate

Although potassium carbonate (K_2CO_3) is less explored as compared to potassium chloride, the corrosivity of potassium carbonate has been found occasionally in the fly ashes from biomass boilers. It has been suggested that the reaction between potassium carbonate and the protective chromia layer is similar to that between potassium chloride and the chromia layer. This is proved by exposing 304L stainless steel to temperature of 500 ℃ and 600 ℃ whereby the protective oxide scales is suffered from chromium depletion due to the formation of potassium chromate according to Equation (2.12) and (2.13). Hence, the 304L stainless steel is said to be less resistant to corrosion (Pettersson et al., 2011).

$$\frac{1}{2}Cr_2O_3 + 2KCl + H_2O + \frac{3}{4}O_2 \rightarrow K_2CrO_4 + 2HCl \quad (2.12)$$

$$\frac{1}{2}Cr_2O_3 + K_2CO_3 + \frac{3}{4}O_2 \rightarrow K_2CrO_4 + CO_2 \quad (2.13)$$

Lehmusto et al. (2012) confirmed the aggressive character of K_2CO_3 toward the chromia-protected steels. The corrosion mechanism for the oxidation of chromia-protected steels starts with the destruction of the protective layer through the reaction with KCl or K_2CO_3, forming K_2CrO_4. Oxidation of the steel may continue when chloride come into contact with the exposed metal surface.

2.3 Mitigation Strategies

In biomass waste boiler with a high content of alkali metal materials, chlorides and low sulphur content will undergo significant corrosion in areas, even at low steam temperature in the vicinity of 500 – 550 ℃ (Nunes et al., 2016). There are some methods that can be taken to prevent and reduce corrosion (Amir et al., 2014), such as design the boiler to control the vapour temperature at which the corrosion rate is acceptable, the use of additives to alter the chemistry of the combustion gases and the deposition of ash, and the selection of higher corrosion resistance alloys to the biomass boiler parts.

2.3.1 Co-combustion

Corrosion can be prevented by the destruction of alkali chlorides before they deposit on superheaters surface because chlorine deposition in the form of alkali chlorides dominates strongly over the deposition of chlorine in other compounds (Aho et al., 2008). In this regard, sulfur-rich fuels can be properly mixed with chlorine-rich biomasses to prevent chlorine deposition. Aluminum–silicates also act through the similar mechanism.

Aho and Silvennoinen (2004) studied the prevention of chlorine deposition by co-combusting biomass fuels. The fuels were selected based on the elemental composition and the purpose of achieving stoichiometric relations that favor the sequestration of alkalis from the alkali chlorides, according to Equation (2.10) and (2.14), where M = K, Na:

$$Al_2O_3 \cdot SiO_2 + 2MCl + H_2O \rightarrow M_2O \cdot Al_2O_3 \cdot 2SiO_2 + 2HCl \quad (2.14)$$

Pine bark, agricultural waste (AGW) and pulp sludge were the fuels chosen in the study. Based on the initial contents of alkali, sulfur, Al_2O_3, chlorine and SiO_2 in the fuels, the authors showed that co-combustion inhibited chlorine deposition especially by the mechanism shown in Equation (2.14).

In another research, Aho and Ferrer (2005) studied the importance of coal ash composition in protecting the boiler against chlorine-induced corrosion during combustion of meat and bone meal. They observed that high content of reactive aluminumsilicate in the coal were beneficial in avoiding chlorine deposition. The formation of alkali aluminosilicates was considered to be the active path of alkali sequestration and effectively prevent alkali chloride deposition. The presence of sulfur did not avoid chlorine deposition evidencing the little effect of the sulfation reaction as compared with the alkali aluminosilicates formation.

2.3.2 Coating

Coating can be applied on superheater tubes and waterwall tubes to protect underneath material from chlorine-induced corrosion. Schütze et al. (2006) studied the key factors for protective coatings for high temperature applications. The phases of coating layer have to be thermodynamically stable in the operating temperature. Interdiffusion between coating layer and substrate is vital in the protective character of the coating layer. This process should occur as slowly as possible in order to avoid premature coating failure. Furthermore, the thermal expansion coefficients of the substrate, coating and oxide layer should be as close as possible to avoid thermal stresses during heating or cooling cycles. In addition, the coating process will also strongly influence the performance of the protective coating layer. A dense and flat splat

structured coating is desired to enhance corrosion resistance at high temperatures because corrosive species usually diffuse through pores and along splat boundaries. A dense and flat splat structure can increase the distance between the coating surface and the coating/substrate interface thereby slow down the corrosion process of the coated substrate (Sidhu et al., 2006).

Hearley et al. (2001) showed that high velocity oxygen fuel (HVOF) thermal spray process produce coatings that acts as effective barrier against high temperature corrosion. This deposition method is frequently reported for the coatings production that resist high temperature corrosion in diverse industrial applications (Verdian et al., 2012, Mohammadi et al., 2012). Due to the intrinsic film characteristics, such as high density, low oxide levels and increased thickness, HVOF sprayed coatings are superior as compared to coatings obtained by other spraying processes.

Kawahara (2007) studied the application of high temperature corrosion resistant coatings under severe corrosive environment. The author applied high durability coating which is TiO_2-Al_2O_3/625 cermet HVOF coating on high temperature superheaters. The author observed remarkably low thickness loss and penetration of corrosive matter. Oksa et al. (2014) also reported that HVOF sprayed coatings provide corrosion protection for low alloy tube materials. In their study, three nickel based thermal spray coatings, which were Ni–24Cr–16.5Mo, Ni–22Crb5Fe–9Mo–4Nb and Ni–22Cr–10Al–1Y, were tested in a 40MW circulating fluidized boiler (CFB) for two years. The uncoated boiler tubes experienced severe corrosion, whereas the thermal spray coatings exhibited excellent corrosion performance.

2.3.3 Formation of Protective Oxide Scales

Corrosion can be prevented or reduced by using steels of high quality. The corrosion resistance of steel can be enhanced by alloying with nickel (Ni) and chromium (Cr). Nickel provides metallurgical stability, improves thermal stability, weldability, resistance to reducing acids and resistance to stress corrosion cracking particularly in chlorides and caustics. In addition, chromium improves resistance to oxidizing corrosive species, high temperature corrosion and sulfidation. It also enhances resistance to pitting and crevice corrosion. The formation of a protective oxide layer consisting of a corundum-type solid solution $(Cr, Fe)_2O_3$, or even pure Cr_2O_3 if the chromium content of the steel is high enough can protect the steel from corrosion (Lehmusto et al., 2012).

As a result, austenitic stainless steel TP347H is widely used in superheater tubes due to its high cost performance. With high content of Ni and Cr in its composition, it exhibits a better corrosion resistance. Ni and Cr can both form dense protective oxide scales that improves the passive performance of steel dramatically. But, in the work by Liu et al. (2014), the main corrosion product of TP347H is Fe-rich oxides. It suffers severe intergranular corrosion and results in failure. A multi-layered corrosion scale formed on TP347H stainless steel in molten alkali chloride salt at temperature of 650 ℃. According to EDX result, (Fe, Ni)-rich compositions are identified as major phases in the corrosion products. The Cr content in the outer corrosion product layer is lower than that in the inner layer. This indicates that the surface protective Cr_2O_3 scale may be destroyed and the corrosion media permeate inwards to corrode substrate alloy. Some Cl is also identified in the inner layer, but none in the outer layer. This finding suggests

that some chlorides form, and they may volatilize or serve as intermediate products to be transformed into oxides at last.

In order to protect the underneath alloy, the oxide layer must have the ability to prevent the penetration of chlorine into the metal surface which supports the active oxidation mechanism. Andersson and Norell (2005) observed that the Sanicro 28 alloy has the lowest corrosion as compared to steel T22, Alloy 310 and Alloy 65 because it has the most compact oxide scale. This was associated with the ability of the continuous oxide layer at preventing the penetration of chlorine inwards into the metal surface. A dense and thin chromium oxide scale, that separated the chlorides from the metal, was observed to be formed on Sanicro 28 alloy. In this regard, the addition of chromium and nickel as alloying elements to iron seems to favor the formation of such a protective scale.

Enestam et al. (2013) reported that grain size of the material may affect the formation of protective layer. This is evidenced by grain boundary corrosion attack on Sanicro 28 was more severely happened than on AISI 347 whereby the grain size for Sanicro 28 and AISI 347 were 125 lm and 42 lm respectively. Fine grain structure eases the formation of protective chromium oxide layer because larger grain boundary area enhances the diffusion along the grains.

Based on the recent study of Dorcheh et al. (2016), stainless steels SS316 and SS347H formed protective oxide scales in molten salt. However, dissolution of the formed oxide scale in the form of alkali ferrite was observed on stainless steels. A linear weight loss with a very slow kinetics was evident for IN625. IN625 also showed the best protective behavior among alloys. Results revealed that a multiphase oxide layer composed of iron–chromium spinel, iron oxides, and sodium ferrite formed on the

stainless steel SS347H while a dense NiO layer was primarily formed on the IN625 surface. The oxide scale on IN625 remains protective for long term immersions. It shows a linear and very slow weight loss due to dissolution in contact with the molten salt.

In the work of Luo et al. (2012), the corrosion rate of 20#steel, TP347H and C22 alloy are compared based on the mass loss measurement as shown in Figure 2.3. From the result, the corrosion rate of materials decreases from 20#steel to TP347H and the C22 alloy in turn. This indicates that the corrosion resistance increases as the Ni and Cr content increase. Besides, the oxide scales developed on both TP347H and C22 alloy consist of the mixed Ni, Fe, and Cr oxides. But, the corrosion scale of TP347H is porous while the corrosion scale of the C22 alloy is compact. Thus, the corrosion scale developed on C22 alloy is more protective as it can prevent the penetration of chlorine into the metal surface.

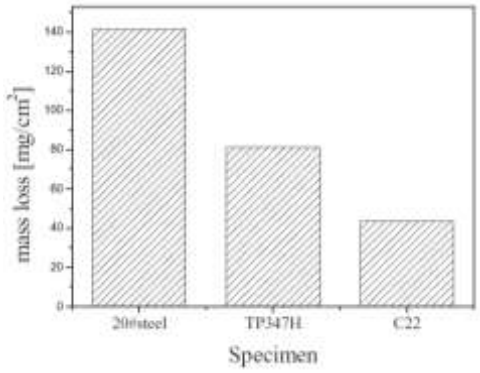

Figure 2.3: Mass losses of 20#steel, TP347H and C22 alloy (Luo et al., 2012)

Furthermore, Mudgal et al. (2016) observed that the Nickel based superalloys showed better corrosion resistance than the cobalt based superalloy under the actual medical waste incinerator where the temperature is more than 1050 ℃. Literatures also have proved that Hastelloy C22 alloy is one of the few materials that are resistant to low

temperature corrosion of seawater (Liu et al., 2014). The composition (in wt%) of the alloy is shown in Table 2.1. The microstructure (Figure 2.4) of Hastelloy C22 shows uniform large equiaxed grains of ~96 μm with some twinning (Chaudhury & Zhao, 1992). Hastelloy C22 alloy (one of Ni–Cr–Mo alloys) are widely studied for its excellent corrosion resistance under extreme conditions, especially for stress corrosion and localized corrosion, such as pitting corrosion, intergranular corrosion and crevice corrosion.

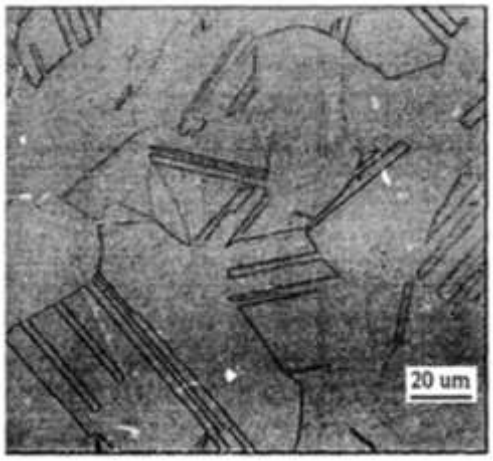

Figure 2.4: As-received microstructure of Hastelloy C22 (Chaudhury & Zhao, 1992)

Table 2.1: Chemical composition of Hastelloy C22 (Chaudhury & Zhao, 1992)

Element	**Ni**	**Cr**	**Mo**	**Fe**	**Mn**	**Co**	**W**	**V**	**Si**	**P**	**C**	**S**
wt%	55.95	21.0	13.3	4.2	0.26	2.02	3.1	0.13	0.027	0.008	0.003	0.002

Liu et al. (2014) stated C22 alloy exhibited high corrosion resistance that results from alloying elements, refined microstructure and oxide mixture of Cr, Fe and Co in the corrosion scale. Figure 2.5 shows the multi-layered corrosion products formed on C22 alloy. The EDS results also reveal a Ni-rich phase in the corrosion products of the alloy and more content of Cr in the inner corrosion product layer (spot B). Figure 2.6

displays the XRD patterns of corrosion products generated on C22 alloy surface. NiO peaks are identified and the high quantity of NiO is confirmed by the EDX analysis. The formation of NiO may be an explanation of the better corrosion resistance of C22 alloy. The protective Cr_2O_3 is also identified at every temperature.

Element	wt%
Ni	83.74
C	08.62
Mo	04.56
Fe	01.53
Cr	01.48
Mn	00.06

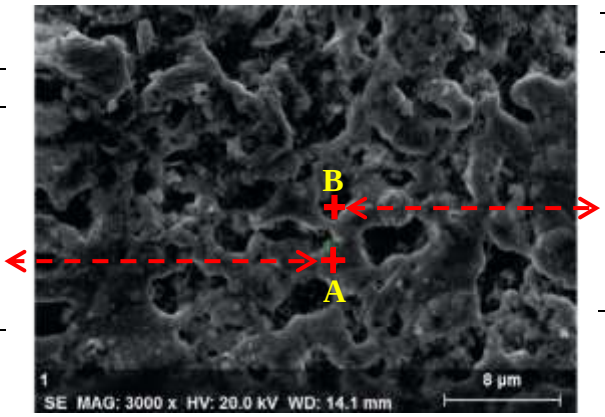

Element	wt%
Ni	43.05
Cr	42.38
Pr	07.55
K	02.01
Mo	01.99
Fe	01.60
O	01.42

Figure 2.5: Surface morphology of corrosion product of Hastelloy C22 corroded in 95.5 wt% KCl and 4.5 wt% NaCl in air for 12 hours at 700 ℃ (Liu et al., 2014)

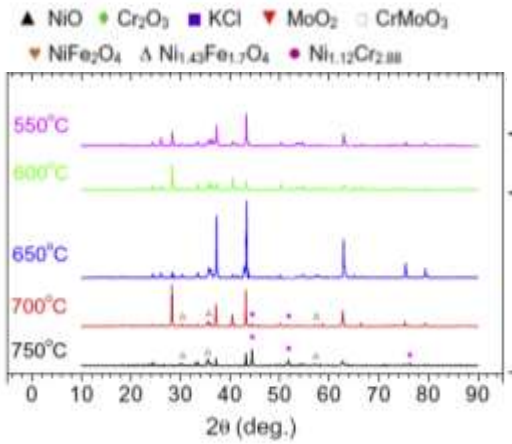

T(℃)	Phase identification
550	$NiO+Cr_2O_3+MoO_2+KCl$
600	$NiO+Cr_2O_3+MoO_2+CrMoO_3+NiFe_2O_4+KCl$
650	$NiO+Cr_2O_3+MoO_2+CrMoO_3+NiFe_2O_4+KCl$
700	$NiO+Cr_2O_3+CrMoO_3+Ni_{1.43}Fe_{1.7}O_4+Cr_{1.12}Ni_{2.28}+KCl$
750	$NiO+Cr_2O_3+CrMoO_3+Ni_{1.43}Fe_{1.7}O_4+Cr_{1.12}Ni_{2.28}$

Figure 2.6: XRD patterns of corrosion products of Hastelloy C22 corroded in 95.5 wt% KCl and 4.5 wt% NaCl in air for 96 hours at 550 – 750 ℃ (Liu et al., 2014)

2.3.3.1 Formation of Chromium Oxide Layer

The selective oxidation of elements that produce a layer of protective scales is the foundation of oxidation protection for alloys that used in high temperature applications. One of the elements that consistently result in protective oxide scales is chromium (Cr). The oxide scale formed is called chromia (Cr_2O_3) layer. Thus, much research has been directed to find alloy compositions that meet other property requirements, such as mechanical property, and also form the protective oxide scales. One of the chromia-forming alloys is nickel-chromium alloy. Alloys in this system even with low Cr contents show internal oxidation of Cr forming Cr_2O_3 islands in a matrix of almost pure Ni. An outer scale of NiO is formed with an inner layer, sometimes porous, of NiO containing $NiCr_2O_4$ islands as shown in Figure 2.7 (Birks et al., 2006).

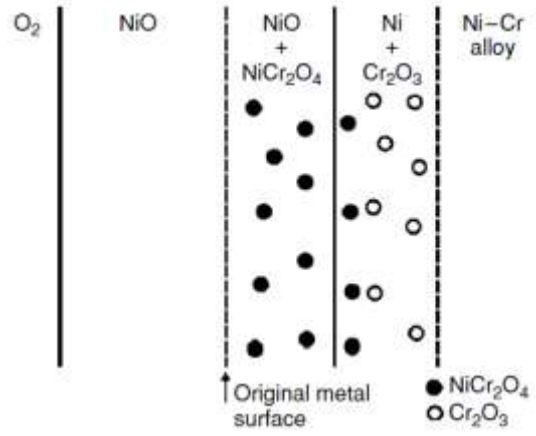

Figure 2.7: Schematic diagram of the oxidation morphology of dilute Ni–Cr alloys (Birks et al., 2006)

As the Cr content increases, to about 10 wt% at 1000 ℃, the oxidation mode changes to produce a complete external scale of Cr_2O_3. At this and higher Cr concentrations the oxidation rate falls abruptly to values more typical of Cr than of Ni. This is illustrated in Figure 2.8.